Surface Curvature and Lateral Pressure Gradient Effects on Laminar Boundary-Layer Separation

G. R. Inger* and B. Dutt†
Virginia Polytechnic Institute and State University, Blacksburg, Va.

An approximate theory is developed for predicting nonsimilar laminar incompressible boundary-layer flow and separation on curved surfaces including lateral pressure gradient and suction effects. The method is based on a generalization of the two-layer flow model of Stratford and Curle. Analytical expressions are obtained for the skin-friction, lateral pressure difference, boundary-layer thickness and separation point location as a function of the shape, pressure and suction distributions. The results are in excellent agreement with exact numerical solutions of the boundary-layer equations for flow around a circular cylinder. Several other practical applications are also discussed, including separation in a linear adverse velocity gradient typical of a wing or compressor blade section and the boundary-layer flow around the nose of a lifting air foil. In all these examples, the longitudinal curvature effect significantly reduces the predicted skin friction and distance to separation.

Nomenclature

a = parameter in inner layer solution
$C_p = 2(p - p_0)/\rho U_{e0}^2$
$C_f = 2\tau_w/\rho U_{e0}^2$
N = parameter in inner solution
p = static pressure
R = longitudinal radius of surface curvature (here approximated as independent of y)
u = velocity component along x
v = velocity normal to surface
x, y = coordinates along and normal to body surface
δ = boundary-layer thickness
μ = coefficient of viscosity
ψ = stream function; location of streamline
ρ = density
τ = shear stress

Subscripts

B = Blasius (flat plate) value
e = conditions at edge of boundary layer
j = location of inner-outer layer interface
L = effective flat plate leading-edge location
m = maximum U_e station
o = start of adverse pressure gradient
s = separation point
w = conditions at wall

Introduction

NONSIMILAR boundary-layer flow and separation in an adverse pressure gradient and the alleviation of separation by the use of suction are extremely important problems in the aerodynamic design of aircraft, missiles and propulsion devices. In particular, the effects of longitudinal surface curvature and the associated lateral pressure variation across the boundary layer can play a significant role near separation. In the case of external flow, for example, these effects arise in the separating boundary-layer region in front of aerodynamic controls such as flaps, jets, etc., as well as in the flow around highly curved segments of lifting wing sections. They are also of great importance in connection with turbomachinery, since the prediction of boundary-layer separation on small highly curved compressor blades can be appreciably influenced by lateral pressure gradient and surface curvature effects.

Presented as Paper 72-368 to AIAA 5th Fluid and Plasma Dynamics Conference, Boston, Mass., June 26, 1972; submitted July 12, 1972; revision received January 23, 1973.

Index categories: Boundary Layers and Convective Heat Transfer—Laminar; Subsonic Flow.

*Professor of Aerospace Engineering. Associate Fellow AIAA.

†Graduate Research Assistant of Aerospace Engineering. Student Member AIAA.

Aside from a few example calculations from finite difference boundary-layer computer programs,[1,2] little has been done in the way of a systematic analysis of these effects in the presence of adverse pressure gradients and suction through the surface. As a first step toward a solution of this problem for the general compressible turbulent case, the present paper examines the combined effects of surface curvature, lateral pressure gradient and suction on the separation of incompressible nonsimilar laminar boundary layers. An approximate analytical treatment incorporating these effects is developed based on a generalization of the two-layered model of boundary-layer flow in adverse pressure gradients originated by Stratford[3] and subsequently refined by Curle.[4] This approach is taken because a) in the absence of the new effects being studied here, this model has been found to yield separation predictions in excellent agreement with a variety of exact numerical solutions and experimental data[4]; b) the model clearly brings out the essential physical features of the flow in a manner amenable to analytical treatment. Unlike the earlier treatments, the lateral pressure gradient and longitudinal streamline curvature are here taken into account.

Following the development of the general theory, application will be made to predicting laminar boundary-layer behavior for some selected example flows for which exact numerical results are available for comparison. In addition, illustrative practical applications are made to the use of suction for separation-delay on curved surfaces, boundary-layer flow around the parabolic leading edge of a wing at angle of attack, and separation in an adverse pressure gradient field typical of a compressor blade section. Finally, possible extensions of the present theory to compressible and/or turbulent flows are briefly discussed.

Development of the General Theory

We consider flows in which the pressure is constant between $x = 0$ and some station $x = x_0$, followed by an arbitrary continuous pressure rise in $x > x_0$ (this zero pressure gradient condition for $x < x_0$ will be subsequently relaxed as shown below). Moreover, the application of suction will be restricted to the pressure rise region. Note that the pressure and skin-friction coefficients used herein are defined in reference to the inviscid flow at x_0:

$$C_p \equiv 2(p - p_0)/\rho U_{e_0}^2 \text{ and } C_f \equiv 2\tau_w/\rho U_{e_0}^2$$

where

$$p_0 = p_e(x_0) \text{ and } U_{e_0} = U_e(x_0)$$

As illustrated schematically in Fig. 1, the boundary-layer thickness for $x > x_0$ is divided into two regions: a

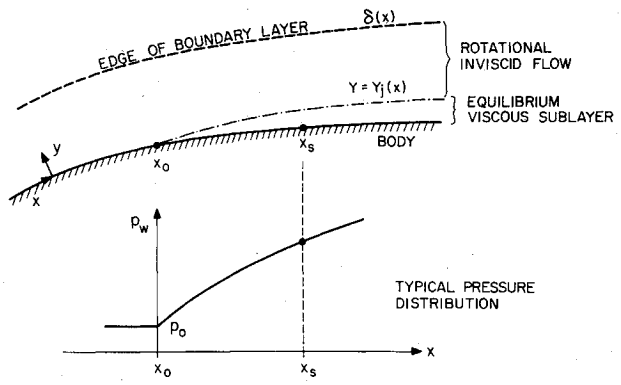

Fig. 1 Schematic of two-layer flow model.

thin local equilibrium sublayer near the (porous) surface where inertia effects are negligible, overlaid by a thick outer layer of essentially rotational inviscid flow with a small viscous total head loss (approximated by the local flat plate value) in which lateral pressure gradient and longitudinal streamline curvature effects are taken into account. Since Stratford and Curle have already discussed in detail the analytical formulation of this model, only a brief outline is given here with emphasis on the new features not included heretofore.

Regarding the nearly-inviscid outer region $y \geq y_j$ where y_j is the height of the interface between the inner and outer layers, the velocity along any streamline x,ψ can be approximated by

$$(u^2)_{x,\psi} = (u^2{}_B)_{x,\psi} - [2(p - p_0)/\rho] \tag{1}$$

where u_B is the Blasius solution without surface mass transfer or pressure gradient. Two successive differentiations of this equation combined with the normal momentum equation $\partial p/\partial y \simeq \rho u^2/R$ and the fact that $u = \partial\psi/\partial y$ then yield the following expressions for the outer velocity profile gradient and curvature, respectively:

$$[\partial u/\partial y]_{x,\psi} = [\partial u_B/\partial y]_{x,\psi} - u/R \tag{2}$$

$$[\partial^2 u/\partial y^2]_{x,\psi} = [u/u_B)\frac{\partial^2 u_B}{\partial y^2}]_{x,\psi} - \frac{1}{R}(\frac{\partial u_B}{\partial y})_{x,\psi} + \frac{u}{R^2} \tag{3}$$

In contrast, the low-speed flow within the thin inner layer $0 \leq y \leq y_j(x)$ has negligible inertia and lateral pressure gradient ($p_w \simeq p_j$) and so can be adequately approximated by the polynomial velocity profile

$$\mu u = \tau_w y + \frac{1}{2}(\frac{dp}{dx} - \frac{\tau_w v_w}{\mu/\rho})y^2 + ay^N \tag{4}$$

where $\tau_w = \mu(\partial u/\partial y)_w$ is the skin friction and the parameters a and $N > 2$ are arbitrary constants which provide matching at $y = y_j$ with the outer solution. The two layers

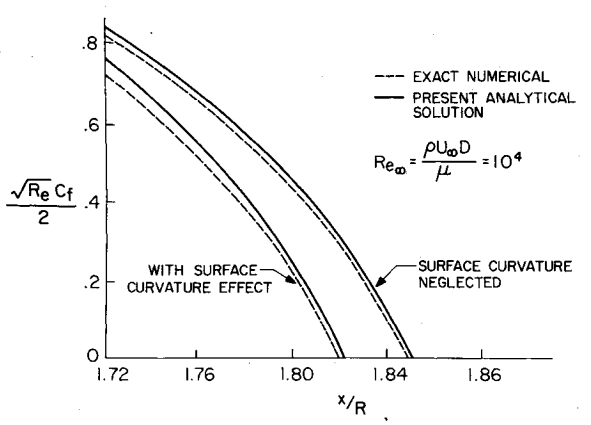

Fig 2 Shear stress distribution around a circular cylinder.

are matched by requiring that ψ, u, $\partial u/\partial y$ and $\partial^2 u/\partial y^2$ each be continuous at $y = y_j$. These four conditions are sufficient to determine τ_w, a, y_j and ψ_j with N appearing as an arbitrary profile parameter (the value $N = 3.043$ recommended by Curle is used here). As in Stratfords original theory,[3] the simplifying assumption is made that the inner layer is sufficiently thin for the Blasius profile to be linear throughout. On this basis, we obtain the following approximate analytical relationship between the skin-friction and surface pressure distributions including the effect of suction, longitudinal curvature and lateral pressure gradient (see Appendix A):

$$x^2\{\frac{dCp_j}{dx} - \frac{2\tau_w v_w}{\mu U_{e_0}{}^2}\}^2\{Cp - \frac{2\tau_{B_w}}{\mu U_{e_0}{}^2}\int_{x_0}^{x} v_w dx\} = 0.0104(1 - \frac{\tau_w}{\tau_{B_w}})^3(1 + 2.02\frac{\tau_w}{\tau_{B_w}}) + \frac{0.0484}{R}\frac{C_{f_B}}{[\frac{dCp}{dx} - (2\tau_w v_w/\mu U_{e_0}{}^2)]}\{\frac{A[1 - (\tau_w/\tau_{B_w})]}{(0.5105)^2} + \frac{B[1 - (\tau_w/\tau_{B_w})]}{0.5105} + C\} \tag{5}$$

where A, B and C are parameters defined in Appendix A. The corresponding inner-layer thickness distribution is given by

$$y_j = (y_j)_{R=\infty}[1 - \frac{1.57\,C_{f_B}/R}{[dCp_j/dx - (2\tau_w v_w/\mu U_{e_0}{}^2)]}(1 + 0.242\tau_w/\tau_{w_B})] \tag{6a}$$

where the solution for an uncurved surface is

$$(y_j)_{R=\infty} \simeq \frac{[1 - (\tau_w/\tau_{w_B})]C_{f_B}}{0.511[dCp_j/dx) - (2\tau_w v_w/\mu U_{e_0}{}^2)]} \tag{6b}$$

It should be noted that the foregoing analysis, although not excluding all accelerated flows, does assume that the initial velocity profile at $x = x_0$ is of the Blasius type. However, boundary-layer flows beginning with a nonzero thickness and/or with a nonzero favorable pressure gradient (such as at a stagnation point) can also be treated by the present theory if one defines the following equivalent flat plate origin x_L following the equivalent momentum thickness method derived by Curle[4]:

$$x_L = x_m - \int_0^{x_m}(\frac{U_e}{U_{e_m}})^5 dx \tag{7}$$

The development of the boundary layer in $x \geq x_m$ may thus still be treated by the foregoing theory provided x is replaced by $x = x - x_L$ and C_f and C_p are defined in terms of the inviscid pressure and velocity at $x = x_m$ instead of at $x = x_0$.

To complete the solution, we determine the pressure change across the outer layer caused by centrifugal force associated with the surface curvature. Combining the normal momentum equation $\partial p/\partial y \simeq \rho u^2/R$ with the outer velocity profile Eq. (1), we find $p - p_0$ to be governed by the nonhomogeneous linear first order differential equation

$$\partial(p - p_0)/\partial y + (2/R)(p - p_0) \simeq \rho u_B{}^2/R \tag{8}$$

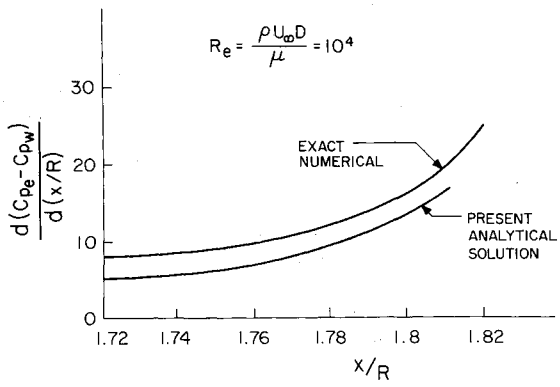

Fig. 3 Lateral pressure change across the circular cylinder boundary layer.

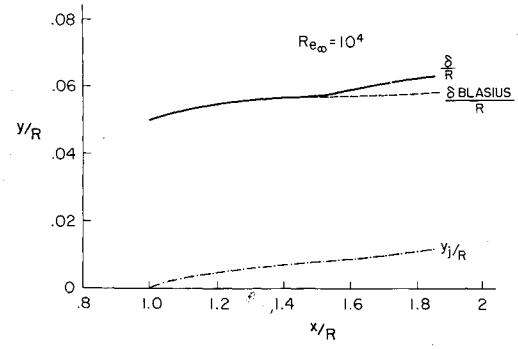

Fig. 4 Boundary-layer and sublayer thicknesses along a circular cylinder.

which integrates to the solution

$$p_e - p_0 = e^{-2\delta/R}(p_w - p_0) + \rho\frac{e^{-2\delta/R}}{R}\int_0^\delta e^{2y/R}u_B^2 dy \quad (9)$$

If we retain only first-order terms in the curvature effect (i.e., in δ/R) and neglect the suction effect on u_B, Eq. (9) can be simplified after evaluating the integral to the final approximate result:

$$Cp_e - Cp_w \simeq (\delta/R)[13.5 - 2(Cp_w - Cp_0)] \quad (10)$$

In conjunction with an appropriate estimate for the boundary-layer thickness which accounts for the adverse pressure gradient region (such as described in Appendix B), Eq. (10) enables a simple calculation of the lateral pressure difference, which involves an outward centrifugal increase slightly diminished by the effect of the adverse pressure gradient term $Cp_w - Cp_0$.

The foregoing analysis provides an approximate analytical description of the skin-friction, equilibrium sublayer thickness and lateral pressure difference distributions along any curved surface for an arbitrary imposed adverse pressure gradient including suction. In particular, it yields a closed form separation point criterion that includes all these effects; setting $\tau_w = 0$ at $x = x_s$, Eq. (5) thus yields

$$x_s^2\left[\frac{dCp}{dx}\right]_s^2\left[Cp_{w_s} - \frac{2\tau_{B_w}}{\mu U_{0_e}^2}\int_{x_0}^{x_s} v_w dx\right] \simeq 0.0104 - \frac{0.655\,C_{f_B}}{(dCp/dx)_s R} \quad (11)$$

which clearly indicates that convex surface curvature ($R > 0$) hastens separation and increases the amount of suction required to delay it. The corresponding inner sublayer thickness at separation is finite and given by Eq. (6b) with $\tau_w = 0$. In the case of flat surfaces ($R \to \infty$), the equation reduces to the result given by Curle[4] upon setting $Cp_w \simeq Cp_e$. Equation (11) is a major result of the present work, since it provides a practical closed form expression that proves very useful in the analysis of the boundary-layer development and separation on highly curved aerodynamic shapes.

Example Applications

Flow around a Circular Cylinder

An important basic flow problem where the new features of the present analysis involving curvature may be illustrated is the case of two-dimensional flow around a circular cylinder. Based on the classical potential inviscid flow velocity distribution $U/U_\infty = (1 - Cp_w)^{1/2} = 2\sin(X/R)$ where here x is the distance around the circumference and R its radius, we get from Eq. (7) that

$$x_L = \frac{\pi}{2} - \int_0^{\pi/2} \sin^5\frac{x}{R}d\left(\frac{x}{R}\right) \simeq 1.038 \quad (12)$$

For a unit diameter Reynolds number of 10^4, the resulting shear stress distributions and separation point locations predicted by the present method both with and without the surface curvature effect are shown in Fig. 2. Also shown in the figure for comparison are the exact numerical results of Bluston and Paulson[2] obtained by a finite difference solution of the complete second-order boundary-layer theory equations. It is seen that the present analytical theory yields very good results, which is especially encouraging in view of its relative simplicity and ease of use. It is also clear from Fig. 2 that longitudinal curvature does indeed have a significant effect on such curved bodies, especially in decreasing the predicted skin friction and distance to separation.

Another interesting feature of the solution, the lateral pressure difference due to curvature, is illustrated in Fig. 3 as the distribution of the axial gradient of this difference around the cylinder. Again, the agreement with Bluston and Paulson's exact results is seen to be good. Evidently, a significant lateral pressure change across the boundary layer can build up as the separation point is approached.

The corresponding growths of the boundary-layer thickness as estimated from Eq. (B2) and inner equilibrium sublayer along the lee side of the cylinder are illustrated in Fig. 4. Near separation, δ and y_j both thicken noticeably as one would expect, implying that viscous-inviscid interaction effects will undoubtedly become important in this region (an extension which includes these effects is currently being developed).

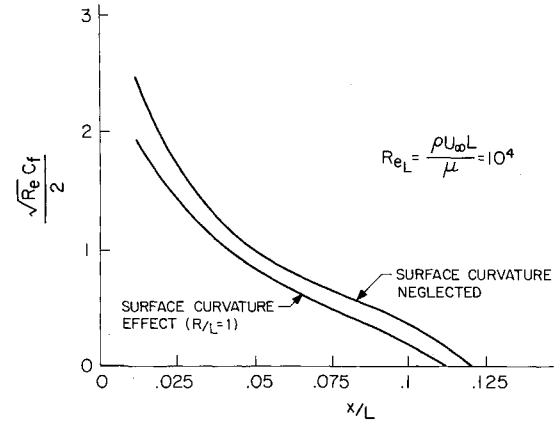

Fig. 5 Shear stress distribution for linearly-retarded flow along a curved surface.

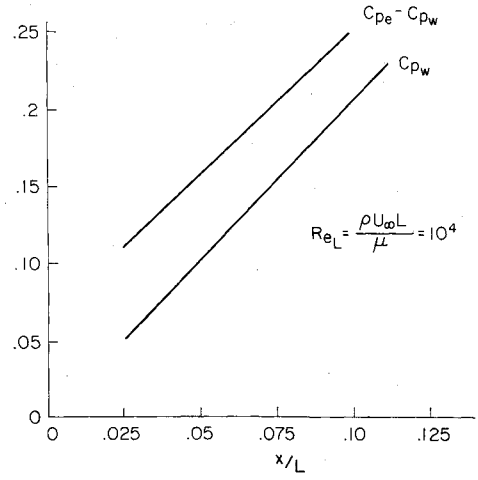

Fig. 6 Lateral pressure change across the linearly-retarded boundary-layer flow.

Linearly-Retarded Flow along a Curved Surface

The Howarth problem[6] of a linearly decelerated inviscid flow $U_e = U_0[1 - (x/L)]$ with $U_0 = U_\infty$ and $Cp = 2x/L - (x/L)^2$ is a useful example because it has been previously studied in some detail without the effect of curvature by Curle, who found that the present two-layer model approach gives very accurate answers when compared with Howarths exact solution.[4]

We consider first the case of a constant wall curvature (R = const) without any suction. Since the flow is everywhere retarded, $x_L = 0$. Choosing an illustrative Reynolds number value $Re_L = 10^4$, the typical effect of convex curvature in causing a decrease in skin friction throughout the length of flow and in hastening separation is illustrated in Fig. 5. The corresponding growth in the lateral pressure difference across the boundary layer associated with the wall curvature, which is rather large in the present example, is shown in Fig. 6. The thickening of both the over-all boundary layer and the equilibrium sublayer as the separation point is approached are shown in Fig. 7 to once again illustrate the likely importance of viscous-inviscid interaction in analyzing the separation process per se.

Another interesting aspect of this "ramp flow" problem is the use of suction to delay separation and the influence of the surface curvature on the amount of such suction required. Assuming a uniform suction distribution along the surface, the separation criterion (11) reduces to

$$\left(\frac{x_s}{L}\right)^2 \left(1 - \frac{x_s}{L}\right)^2 \left[2\frac{x_s}{L} - \frac{x_s^2}{L^2} - 0.664\sigma\left(\frac{x_s}{L}\right)^{1/2}\right] \simeq 0.0026 - \frac{68.5 C_{f_B}}{R/L} \quad (13)$$

where $\sigma = v_w Re_L / U_{o_e}$ is the appropriate nondimensional suction parameter. As expected, suction increases x_s/L, the amount required being increased by the presence of a convex surface curvature. This is illustrated in Fig. 8, where x_s/L is plotted vs σ for several values of surface curvature R/L. The result evident in this figure that sufficiently strong suction can completely suppress separation has been pointed out previously by Curle.[4] Clearly, on highly curved air-foil sections, engineering analyses regarding the use of suction should take into account the curvature effects for conservative design estimates.

Flow around a Parabolic Leading Edge at Angle of Attack

The case of laminar boundary-layer flow around a parabola at angle of attack is of practical importance because it closely simulates the problem of flow around the highly curved leading-edge region of a wing section at high lift. Owing to the large nose curvatures involved, it is of interest to appraise the longitudinal curvature effect on the boundary-layer development around the nose. The present theory provides a means of doing this.

Based on the inviscid velocity distribution given by Van Dyke,[7] the present theory has been used to calculate the skin-friction distribution around a parabolic nose both with and without the longitudinal curvature effects; the results are shown in Fig. 9 for a typical angle of attack situation. Also shown for comparison is an exact numerical solution of the boundary-layer equations neglecting curvature obtained by Werle and Davis,[8] in order to once again illustrate the excellent engineering accuracy of the present approximate theory. It is seen from Fig. 9, that the separation-hastening surface curvature effects in this flow problem can be very significant indeed; their neglect can cause a substantial overestimate of the skin-friction level and separation distance (and hence an underestimate of the form drag contribution to total drag). Clearly, numerical boundary-layer computer programs used for air-foil design optimization studies should include an account of these curvature effects.

Flow around a Compressor Blade Section

Another important application of the present theory is to the prediction of boundary-layer separation on small highly curved blades found in turbomachinery. As an illustrative example, we consider a compressor blade air-foil section in the NACA 65-series under a typical design operating condition of 12.4° angle of attack at a chord Reynolds number of 0.25×10^6. A sketch of this section and the experimental pressure distribution along the suction side obtained by Westphal and Godwin[10] are given in Fig. 10. Inspection of all the pressure distribution data in Ref. 10 reveals that a small region of zero pressure gradient occurs at approximately 20% chord over a wide range of angles of attack. Thus, as a first approximation in applying our theory, this location is taken to be the effective flat plate leading edge x_L. Downstream, the pressure distribution may be conveniently approximated reasonably well by a linear increase; in the example of Fig. 10, we used $Cp_\infty \simeq 1.9 - 1.4\,(x/C)$ along the upper surface, where in this adverse pressure gradient region, the convex surface curvature is approximately constant with the value $R \simeq 3.5\,C$.

The predicted skin-friction distributions along the upper blade surface with and without the surface curvature effects are shown in Fig. 11. To be sure, the actual

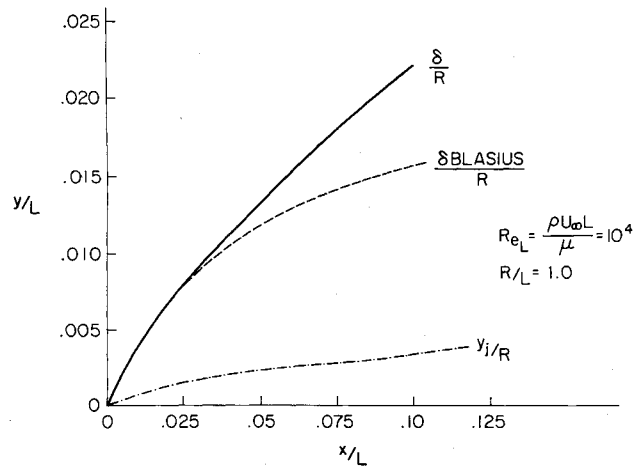

Fig. 7 Boundary-layer and sublayer growth for the linear-retarded flow.

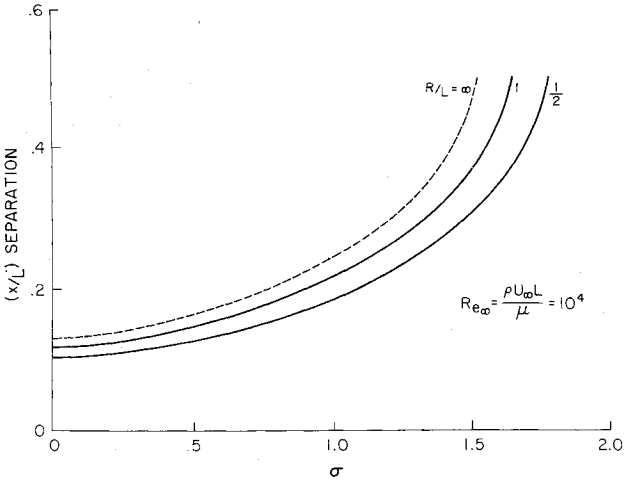

Fig. 8 The effects of suction and curvature on the separation point in linearly-retarded flow.

boundary-layer flow in this particular example (as is often the case in turbomachinery blade problems) is likely turbulent rather than laminar, so that the present theory is not really applicable quantitatively; nevertheless, this example does illustrate the general magnitude and character of the new longitudinal surface curvature and lateral pressure gradient effects (Fig. 11 clearly indicates the importance of taking these effects into account to obtain conservative aerodynamic design estimates regarding the influence of boundary-layer separation). Moreover, there are some lower Reynolds number conditions arising in turbomachinery applications (as well as in optimum air-foil shape studies[9]) where laminar flow does in fact prevail and the present theory is directly applicable.

Conclusions

Although approximate, the present theory has the virtues of a) sound physical modelling of the essential flow features, b) yielding results in relatively easy-to-use analytical form, and c) good engineering accuracy. As such, it may be employed in either of two ways. First, it can be used to estimate the boundary-layer characteristics and separation point on bodies with given pressure and curvature distributions. Secondly, the present theory can be used with particular convenience (because of its analytic form) in so-called "design problem" studies where one varies the shape and pressure distributions so as to optimize some gross property (e.g., maximize x_s).

Another merit of the present two-layered analysis is that it may be generalized to include compressibility effects, heat transfer, and the presence of a turbulent

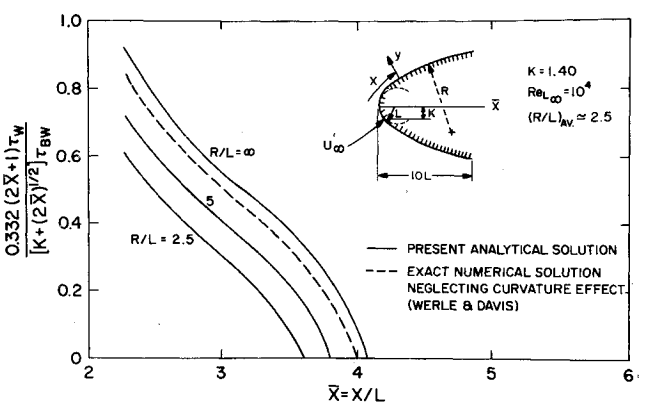

Fig. 9 Shear stress distribution around a parabolic leading edge at angle of attack.

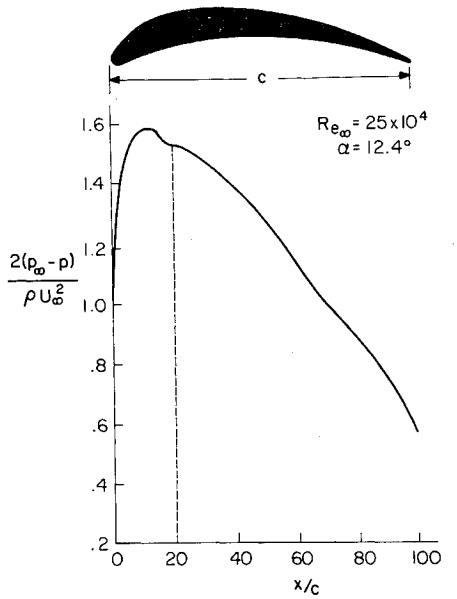

Fig. 10 Compressor blade section and lee side pressure distribution (NACA 65-series).

boundary layer. This is important, for example, in view of Thomann's[11] results that surface curvature can have a very significant influence on heat-transfer characteristics, especially when the boundary layer is turbulent. Although such a generalization is beyond the scope of the present paper, we may briefly outline the approach involved. The outer quasi-inviscid flow layer can be treated similarly to the incompressible case, now however using the compressible form of the Bernouli equation plus the "compressible form" of a suitable flat plate turbulent boundary-layer profile (say a "Law of the Wake" profile) with which to estimate the total head loss along streamlines. The corresponding total enthalpy loss in the nonadiabatic case can be determined from Crocco's energy equation integral. Regarding the inner layer, the analysis proceeds in a manner similar to Stratfords original work[12] with a better viscosity model and with allowance for compressibility and heat transfer being made following Van Driest's pioneering treatment of the compressible "Law of the Wall" region[13] (within which we assume the inner layer resides). The major difficulty encountered here is the current lack of a suitable turbulent eddy viscosity model in strong adverse pressure gradients with small wall shear[14]; otherwise, a generalized mixing length model following the line suggested by Cebeci[15] should probably suffice for most engineering purposes.

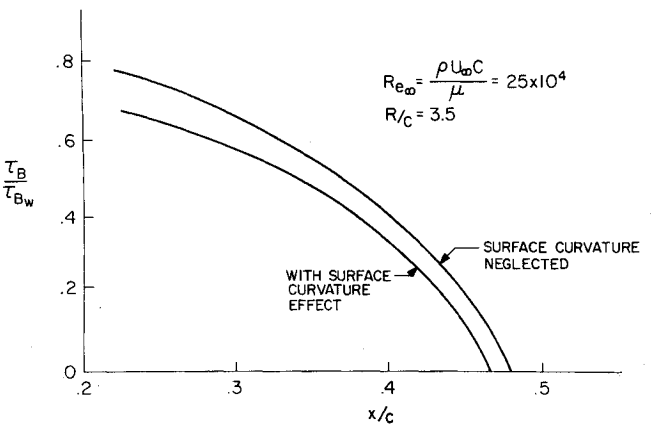

Fig. 11 Predicted shear stress distribution and separation location on the compressor blade.

Appendix A

For the purpose of illustrating the essential steps in deriving the desired relationships, we will neglect here the effect of suction. Then letting $\bar{A} \equiv a y_j^{N-2}$, the inner-outer matching of $\partial u/\partial y$ and $\partial^2 u/\partial y^2$ at $y = y_j$ yields the pair of equations

$$\tau_{B_w} = \tau_w + \left(\frac{dp}{dx}\right)_j y_j + N\bar{A}y_j + \frac{1}{R}\left[\tau_w y_j + \frac{y_j^2}{2}\left(\frac{dp}{dx}\right)_j^2 + \bar{A}y_j^2\right] \quad \text{(A1)}$$

$$\left(\frac{dp}{dx}\right)_j + N(N-1)\bar{A} + \frac{\tau_{B_w}}{R} - \frac{1}{R^2}\left[\tau_w y_j + \frac{y_j^2}{2}\left(\frac{dp}{dx}\right)_j^2 + \bar{A}y_j^2\right] = 0 \quad \text{(A2)}$$

Dividing Eq. (A1) by R, adding to Eq. (A2) and solving for $\bar{A}$ gives

$$\bar{A} = -\frac{\{[1 + (y_j/R)](dp/dx)_j + \tau_w/R\}}{N[(N-1) + (y_j/R)]} \quad \text{(A3)}$$

which upon substituting back into Eq. (A1), neglecting terms of order $(y_j/R)^2$ compared to unity and approximating the coefficients of terms involving R^{-1} by their flat surface ($R = \infty$) values yields for $N = 3.043$ the Eqs. (6a) and (6b) cited in the text.

The corresponding skin-friction pressure-distribution relationship is derived as follows. Substituting Eq. (4) and the value of ψ_j given by the y-integral of Eq. (4) plus Eq. (A3) into Eq. (1) yields

$$C_p U_e^2 \mu^2 = 2\tau_{B_w}\left[\frac{\tau_w}{2}\left\{\frac{\tau_{B_w}\left(1 - \frac{\tau_w}{\tau_{B_w}}\right) - \frac{\mu u_j}{R}}{\frac{N-2}{N-1}\left(\frac{dp}{dx}\right)_j - \frac{\tau_B}{(N-1)R}}\right\} + \left\{\frac{\tau_{B_w}\left(1 - \frac{\tau_w}{\tau_{B_w}}\right) - \frac{\mu u_j^3}{R}}{\frac{N-2}{N-1}\left(\frac{dp}{dx}\right)_j - \frac{\tau_{B_w}}{(N-1)R}}\right\}\left\{\frac{N(N^2-1) - 6}{6N(N^2-1)}\frac{dp}{dx}_j - \frac{\tau_{B_w}}{N(N^2-1)R}\right\}\right] - \left[\tau_w\left\{\frac{\tau_{B_w}\left(1 - \frac{\tau_w}{\tau_{B_w}}\right) - \frac{\mu u_j}{R}}{\frac{N-2}{N-1}\left(\frac{dp}{dx}\right)_j - \frac{\tau_B}{(N-1)}\frac{1}{R}}\right\} + \left\{\frac{\tau_B\left(1 - \frac{\tau_w}{\tau_{B_w}}\right) - \frac{\mu u_j^2}{R}}{\frac{N-2}{N-1}\frac{dp}{dx}_j - \frac{\tau_{B_w}}{(N-1)R}}\right\}\left\{\frac{(N-2)(N+1)}{2N(N-1)}\left(\frac{dp}{dx}\right)_j - \frac{\tau_B}{N(N-1)R}\right\}\right]^2 \quad \text{(A4)}$$

Furthermore Eq. (4) at y_j can also be written with help of Eq. (A3) as

$$u_j = \frac{\tau}{\mu}y_j + \frac{y_j^2}{2\mu}\left(\frac{dp}{dx}\right)_j\left[1 - \frac{2}{N(N-1)}\left\{1 + \frac{y_j}{R}\left(\frac{N-2}{N-1}\right)\right\}\right] \quad \text{(A5)}$$

Then combining Eqs. (A4) and (A5) and simplifying along the lines discussed in the foregoing paragraph, we obtain after considerable algebraic rearrangement:

$$x^2 Cp\left(\frac{dCp}{dx}\right)^2 = 0.0104\left(1 - \frac{\tau_w}{\tau_{B_w}}\right)^3\left(1 + 2.02\frac{\tau_w}{\tau_{B_w}}\right) + \frac{0.0484}{R}\frac{C_{f_B}}{\left(\frac{dCp}{dx}\right)}\left\{\frac{A[1 - (\tau_w/\tau_{B_w})]^2}{(0.5105)^2} + \frac{B[1 - (\tau_w/\tau_{B_w})]}{(0.5105)} + C\right\} \quad \text{(A6)}$$

$$A = \frac{\tau_w}{\tau_{B_w}}\left(1 - \frac{\tau_w}{\tau_{B_w}}\right)^2\left(\frac{N-2}{N-1}\right)^2\left[N^2 - \frac{2N^2}{N(N-1)}\right] + \left(1 + \frac{\tau_w}{\tau_{B_w}}\right)^2\left(\frac{N-1}{N-2}\right)^3\left[N^2 - \frac{2N^2}{N(N-1)}\right]\left[\frac{N(N^2-1)-6}{2N(N^2-1)}\right] - \left(\frac{\tau_w}{\tau_{B_w}}\right)^2\left(1 - \frac{\tau_w}{\tau_{B_w}}\right)\left(\frac{N-1}{N-2}\right)^2\left[N^2 - \frac{2N^2}{N(N-1)}\right] - \left(\frac{\tau_w}{\tau_{B_w}}\right)^3\left(\frac{N-1}{N-2}\right)^2(N+1)\left[N^2 - \frac{2N^2}{N(N-1)}\right]\left(\frac{1}{2N^2}\right) - \left(\frac{\tau_w}{\tau_{B_w}}\right)^2\left(1 - \frac{\tau_w}{\tau_{B_w}}\right)^2(N+1)\left[N^2 - \frac{2N^2}{N(N-1)}\right]\frac{1.5}{N}$$

$$B = 2\left(\frac{\tau_w}{\tau_{B_w}}\right)^2\left(1 - \frac{\tau_w}{\tau_{B_w}}\right)\left(\frac{N-1}{N-2}\right)^2 + \left(\frac{\tau_w}{\tau_{B_w}}\right)\left(1 - \frac{\tau_w}{\tau_{B_w}}\right)^2\left(\frac{N-1}{N-2}\right)^3\left[\frac{N(N^2-1)-6}{N(N^2-1)}\right] - 2\left(\frac{\tau_w}{\tau_{B_w}}\right)^3\left(1 - \frac{\tau_w}{\tau_{B_w}}\right)\left(\frac{N-1}{N-2}\right)^2 - \left(\frac{\tau_w}{\tau_{B_w}}\right)\left(1 - \frac{\tau_w}{\tau_{B_w}}\right)^3\left(\frac{N-1}{N-2}\right)^2\left(\frac{N+1}{N}\right)^2 - 3\left(\frac{\tau_w}{\tau_{B_w}}\right)^2\left(1 - \frac{\tau_w}{\tau_{B_w}}\right)^2\left(\frac{N-1}{N-2}\right)^2\left(\frac{N+1}{N}\right)$$

$$C = \left(\frac{\tau}{\tau_{B_w}}\right)\left(1 - \frac{\tau}{\tau_{B_w}}\right)^2\left(\frac{N-1}{N-2}\right)^2\frac{2}{(N-2)} + \left(1 - \frac{\tau}{\tau_{B_w}}\right)^3\left\{\left(\frac{N-1}{N-2}\right)^3\left[\frac{N(N^2-1)-6}{N(N-2)(N^2-1)}\right] - \left(\frac{N-1}{N-2}\right)^3\left(\frac{2}{N(N^2-1)}\right)\right\} - \left(\frac{\tau}{\tau_{B_w}}\right)\left(1 - \frac{\tau}{\tau_{B_w}}\right)^2\left(\frac{N-1}{N-2}\right)^2\frac{2}{(N-2)} - \left(1 - \frac{\tau}{\tau_{B_w}}\right)^4\left(\frac{N-1}{N-2}\right)^4\left[\frac{(N-2)(N+1)^2}{2(N^2)(N-1)^2} - \frac{(N-2)(N+1)}{N^2(N-1)^2}\right] + \left(\frac{\tau}{\tau_{B_w}}\right)\left(1 - \frac{\tau}{\tau_{B_w}}\right)^3\left\{\left(\frac{N-1}{N-2}\right)^3\frac{2(N+1)}{N(N-1)} - \frac{(N-1)^3}{(N-2)^3}\frac{3}{N(N-1)}\right\} + \left(\frac{\tau}{\tau_{B_w}}\right)\left(1 - \frac{\tau}{\tau_{B_w}}\right)^3\left(\frac{N-1}{N-2}\right)^3\left(\frac{N+1}{N(N-1)}\right)$$

in which the $R = \infty$ values of τ are to be used. At separation $\tau_w = 0$, these parameters take on the following values for $N = 3.043$: $A = -3.566$, $B = 0$, $C = -0.00000437 \approx 0$.

Appendix B

To circumvent the use of an integral method solution for $\delta(x)$ using the present composite inner-outer velocity profile, an alternative analytical rough estimate can be derived as follows. To the order of accuracy of our outer region solution, the velocity fields with and without curvature have the same streamline ψ; since this must include the edge of the boundary layer, we have $\psi(\delta,x) \approx \psi_B(\delta_B,x)$ or

$$\int_{x_0}^{x} \frac{v_w}{U_{e_0}} dx + \int_0^{\delta} \frac{u}{U_{e_0}} dy \simeq \int_0^{\delta_B} \frac{u_B}{U_{e_0}} dy \qquad \text{(B1)}$$

thereby providing a means of relating δ with pressure gradient to the Blasius value $\delta_B(x)$. Now taking the edge of the boundary layer to be at $\eta_B \simeq 5.00$ in the Blasius similarity variable η_B, the right side of (B1) can be written as $0.20\ \delta_B \int_0^5 (u_B/U_{e0}) d\eta_B$. On the other hand, breaking up the left side integral into contributions from the inner and outer layers, respectively, using Eq. (4) in the outer contribution and converting the integration variable to η_B, we obtain from Eq. (B1) the following approximate expression for δ/δ_B:

$$\frac{\delta}{\delta_B} \simeq \frac{\int_0^5 \frac{u_B}{U_{e_0}} d\eta_B - \frac{5}{\delta_B}\left[\int_{x_0}^{x} \frac{v_w}{U_{e_0}} dx + y_j \int_0^1 \frac{U\,\text{inner}}{U_{e_0}} d(y/y_j)\right]}{\int_{\eta_{B_j}}^5 [(u_B/U_{e_0})^2 - Cp(x)]^{1/2} d\eta_B} \qquad \text{(B2)}$$

Now the first integral in the numerator can be rewritten as the sum

$$\int_{\eta_{B_j}}^5 (u_B/U_{e_0}) d\eta_B + (5/\delta_B) y_j \int_0^1 \frac{u_B}{U_{e_0}} d(y/y_j)$$

Both the last term of this sum and the last integral in the numerator of Eq. (B2) can then be represented for purposes of a first approximation by a linear velocity variation, giving

$$\int_0^1 \frac{U\,\text{inner}}{U_{e_0}} d\left(\frac{y}{y_j}\right) \simeq \frac{\tau_w y_j}{2\mu U_{e_0}} \qquad \text{(B3)}$$

On the other hand, the denominator of Eq. (B2) can be treated in an approximate closed form manner as follows. For the sole purpose of evaluating its ratio to

$$\int_{\eta_{B_j}}^5 (u_B/U_{e_0}) d\eta_B$$

we can approximate $u_B(\eta)$ by the linear function $u_B = U_{e_0} f_{B_w}'(\eta_B)$ for $0 \le \eta_B \le (f_{B_w}')^{-1}$, $u_B = U_{e_0}$ for $\eta_B > (f_{B_w}'')^{-1}$ where $f_{B_w}' \cong 0.47$. In this way, we get upon neglecting terms in $\eta_{B_j} f_{B_w}'$ as small that the aforementioned ratio of integrals is approximately equal to $[1 - Cp(x)]^{1/2}$. Introducing all these approximations into Eq. (B2), we finally obtain the following engineering estimate of the boundary-layer thickness compared to the local flat plate value δ_B:

$$\frac{\delta}{\delta_B} \simeq [1 - (5\int_{x_0}^{x} \frac{v_w}{U_{e_0}} dx)/(\delta_B \int_0^5 \frac{u_B}{U_{e_0}} d\eta_B)][1 - C_p(x)]^{-1/2}$$

References

[1]Davis, R. T., Whitehead, R. E., and Wornom, S. F., "The Development of an Incompressible Boundary Layer Theory Valid to Second Order," E-70-1, Jan. 1971, Virginia Polytechnic Inst. and State University, Blacksburg, Va.

[2]Bluston, H. S. and Paulson, R. W., "Non-Similar Second Order Boundary Layer Solutions for Subsonic Flow over Curved Surfaces," *Journal de Mechanique*, Vol. 10, June 1971, pp. 163–189.

[3]Stratford, B. S., "Flow in the Laminar Boundary Layer Near Separation," British R&M 3002, Nov. 1954, Her Majesty's Stationary Office, London, England.

[4]Curle, N., "Estimation of Distributed Suction," *Aeronautical Quarterly*, Vol. XI, Feb. 1960, pp. 1–21.

[5]Thwaites, B., "Approximate Calculation of the Laminar Boundary Layer," *Aeronautical Quarterly*, Vol. I, Nov. 1949, pp. 245–252.

[6]Howarth, L., "On the Solution of the Laminar Boundary Layer Equations," *Proceedings of the Royal Society*, Pt. A, Vol. 164, 1938, pp. 542–543.

[7]Van Dyke, M., "Second-Order Subsonic Airfoil Theory Including Edge Effects," TR 1274, 1956, NASA.

[8]Werle, M. S. and Davis, R. T., "Incompressible Laminar Boundary Layers on a Parabola at Angle of Attack: A Study of the Separation Point," *Transactions of the ASME: Journal of Applied Mechanics*, Vol. 2, March 1972, pp. 7–12.

[9]Fink, D. E., "New Airfoil Design Method Developed," *Aviation Week and Space Technology*, Nov. 13, 1972, pp. 45–46.

[10]Westphal, W. R. and Godwin, W. R., "Comparison of NACA 65-Series Compressor Blade Pressure Distributions," TN 3806, 1951, NACA.

[11]Thomann, H., "Effects of Streamwise Wall Curvature on Heat Transfer in a Turbulent Boundary Layer," *Journal of Fluid Mechanics*, Vol. 33, Pt. 2, 1968, pp. 283–292.

[12]Stratford, B. S., "Prediction of Turbulent Boundary Layer Separation," *Journal of Fluid Mechanics*, Vol. 5, 1959, pp. 1–16.

[13]Van Driest, E. R., "Compressible Turbulent Boundary Layers," *Journal of the Aeronautical Sciences*, Vol. 18, 1951, pp. 145–153.

[14]Alber, I. E., "Similar Solutions for a Family of Separated Turbulent Boundary Layers," AIAA Paper 71-203, New York, 1971.

[15]Cebeci, T., "Calculation of Compressible Turbulent Boundary Layer with Heat and Mass Transfer," *AIAA Journal*, Vol. 9, No. 6, June 1971, pp. 1091–1097.